

Published in final edited form as:

*J Magn Reson Imaging*. 2014 December ; 40(6): 1392–1399. doi:10.1002/jmri.24490.

## A variable spatio-temporal resolution 3D Dixon sequence for rapid dynamic contrast enhanced breast MRI

Manojkumar Saranathan, PhD<sup>1</sup>, Dan W. Rettmann, BS<sup>2</sup>, Brian A. Hargreaves, PhD<sup>1</sup>, Jafi A. Lipson, MD<sup>1</sup>, and Bruce L. Daniel, MD, PhD<sup>1</sup>

<sup>1</sup>Department of Radiology, Stanford CA USA

<sup>2</sup>Applied Science Laboratory, GE Healthcare, Rochester MN, USA

### Abstract

**Purpose**—To investigate a new variable spatio-temporal resolution dynamic contrast-enhanced (DCE) MRI method termed Differential Subsampling with Cartesian Ordering (DISCO), for imaging of breast cancer.

**Materials and Methods**—DISCO combines variable density, pseudo-random k-space segmentation and two-point Dixon fat-water separation for high spatio-temporal resolution breast DCE MRI. During the contrast wash-in phase, view sharing is used to achieve high temporal resolution.

Forty patients referred for breast MRI were imaged, 26 using the proposed DISCO sequence and 14 using a conventional low-spatial-resolution dynamic sequence (VIBRANT-FLEX) on a 3T scanner. DISCO dynamic images from 14 patients were compared to VIBRANT-FLEX images from 14 other patients. The image quality assessed by radiologist image ranking in a blinded fashion, and the temporal characteristics of the two sequences were compared.

**Results**—A spatial resolution of  $1.1 \times 1.1 \times 1.2 \text{ mm}^3$  (160 slices, 28 cm FOV) was achieved with axial bilateral coverage in 120s. Dynamic images with ~9s effective temporal resolution were generated during the two-minute contrast wash-in phase. The image quality of DISCO dynamic images ranked significantly higher than low spatial resolution VIBRANT-FLEX images (19.5 vs. 9.5, Mann-Whitney U-test  $p = 0.00914$ ), with no significant differences in the maximum slope of aortic enhancement.

**Conclusion**—DISCO is a promising variable-spatio-temporal-resolution imaging sequence for capturing the dynamics of rapidly enhancing tumors as well as structural features post-contrast. A near 1-mm isotropic spatial resolution was achieved with post-contrast static phase images in 120s and dynamic phase images acquired in 9s per phase.

### Keywords

Dynamic contrast enhanced breast MRI; Variable spatio-temporal resolution; Time resolved imaging; Dixon fat-water separation

## Introduction

Dynamic contrast enhanced MRI (DCEMRI) is commonly used for detection and characterization of malignancies in the breast. However, sub-optimal compromises are often made between temporal and spatial resolution in conventional breast DCEMRI [1]. A high spatial resolution is required to characterize lesion morphology whereas a high temporal resolution is required to accurately characterize contrast uptake both for semi-quantitative and quantitative analysis of contrast enhancement kinetics. Conventional clinical breast DCEMRI often falls into either high spatial (low temporal) resolution *or* high temporal (low spatial) resolution regimes [1–2], although high spatial resolution imaging is increasingly being used. The American College of Radiology (ACR) guidelines recommend 1 mm in-plane spatial resolution, slice thickness of 3 mm or less and enhancement data acquired at intervals spaced 120s or less (<http://www.acr.org/Quality-Safety/Standards-Guidelines>).

Various methods have been proposed to address the spatio-temporal resolution tradeoff in DCEMRI and MR angiography. Earlier two-dimensional keyhole-based methods [3,4] suffered from increased blurring and ghosting artifacts in regions where rapid dynamic changes occur, limiting diagnostic accuracy [4]. Several schemes based on *k-t* segmentation have recently been proposed for time resolved imaging and demonstrated for use in high spatio-temporal resolution MR angiography (MRA). Time Resolved Imaging of Contrast KineticS (TRICKS) [5] and Cartesian Acquisition with Projection Reconstruction like sampling (CAPR) [6] segment elliptically ordered 3D *k*-space into annular or radial regions and time interleave the acquisition of central and peripheral regions to achieve higher temporal resolution. Highly constrained back projection (HYPR) [7] imaging employs radial undersampling and a time-averaged composite image to constrain the reconstruction of the subsampled data, eliminating streaking artifacts. Adaptive radial *k*-space methods like projection reconstruction with TRICKS [8] and *k*-space weighted image combination (KWIC) [9] have been proposed for bilateral breast DCEMRI, where a variable number of radial views are used to reconstruct images with the desired spatio-temporal resolution.

For breast imaging in a clinical setting, a 3D RF-spoiled gradient recalled echo (SPGR) sequence with fat suppression and parallel imaging is still the most commonly used imaging method. The typical temporal resolution of this sequence is 90–120s for an isotropic spatial resolution of 1 mm<sup>3</sup>. While the spatial resolution is tailored for delineation of fine structures and tumor morphology, the lower temporal resolution makes it difficult to characterize wash-in and wash-out kinetics using either semi-quantitative or quantitative models, which typically require a temporal resolution of 10–15s or better in order to capture the fast dynamics of tumor enhancement and account for inter-patient variations of bolus arrival times in the breast [10].

In addition to spatiotemporal resolution, uniform fat suppression is critical for breast imaging. This is more relevant at higher field strengths, where fat suppression can be challenging due to increased B<sub>1</sub> heterogeneity effects. Breast geometry poses a challenge for effective shimming, making it hard to achieve uniform B<sub>0</sub> homogeneity across both breasts and causing traditional fat suppression techniques to perform poorly. Conventional fat suppression techniques apply inversion or saturation pulses centered on the lipid resonance

followed by acquisition of multiple lines of k-space in order to restrict scan times. In breast MRI, this may result in incomplete fat suppression or even inadvertent suppression of the water signal. Variants of the fat-water separation method originally proposed by Dixon [11], such as the 3-point Dixon based IDEAL (Iterative Decomposition of water and fat with Echo Asymmetry and Least-squares estimation) [12] and the 2-point based MEDAL (Multi-Echo with 2-Point Dixon Reconstruction for Decomposition of Aqua/Lipid) [13], have been shown to be robust and relatively immune to the effects of  $B_0$  heterogeneity. The elimination of magnetization preparation pulses provides these Dixon-based methods complete flexibility in the order of k-space acquisition, enabling the use of elliptical centric or other novel k-space ordering approaches without time penalty.

Recently, Pinker et al. [14] presented a 3T fat suppressed breast MRI technique with *separate* low spatial resolution VIBE acquisitions during the contrast wash-in and wash-out phases (13s temporal resolution) and a high spatial resolution VIBE acquisition with conventional fat suppression at peak contrast (120s temporal resolution). “One shot” methods, where the dynamic and the high resolution images are acquired in a single acquisition are advantageous, as they minimize inter scan delays as well as ensure constancy of parameters such as receiver gains, receiver bandwidth, TE/TR for accurate quantitative imaging. One such method for variable spatio-temporal resolution 3T breast DCEMRI using a Dixon fat-water separation scheme was recently presented [15], where only a fraction of elliptically ordered k-space was acquired during the wash-in phase and complete k-space was acquired following peak contrast. This method suffers from image blurring and Gibbs ringing artifacts due to zero-filling without a windowing filter in the high temporal resolution wash-in phases.

The purpose of this study was to demonstrate clinical feasibility of a new high spatio-temporal resolution DCEMRI technique, called DISCO (Differential Sub-sampling with Cartesian Ordering) DCE, that combines a dual-echo SPGR sequence with Dixon fat-water separation, pseudo-random variable density k-space segmentation and a view sharing reconstruction. The sequence seamlessly switches between high temporal/moderate spatial resolution mode during the dynamic contrast wash-in phase and high spatial/low temporal resolution mode during the post-contrast phase, providing variable spatio-temporal resolution in a single acquisition.

## Materials and Methods

### Pulse sequence

A variable density k-space under-sampling scheme was used to generate a pseudo-random distribution of k-space points [16]. All  $k_y$ - $k_z$  points are first sorted in the order of increasing  $k_r = (k_y^2 + k_z^2)$  and then segmented into  $N$  annuli based on  $k_r$  and each annulus  $i$  under-sampled by a factor of  $S_i$  (typically  $S_i \geq i$ ). The central region is fully sampled and the outer annuli increasingly under-sampled by retaining every  $S_i^{\text{th}}$  sample, with different sampling patterns generated by staggering the starting sample. We call this method Differential Sub-sampling with Cartesian Ordering or DISCO. All k-space points are still confined to a Cartesian grid, speeding image reconstruction. The DISCO segmentation can also be applied after undersampling the k-space data for parallel imaging without any

modifications. Since each sub-region is ordered in increasing  $k_r$  as well as smoothed azimuthally to minimize jumps in k-space, eddy current artifacts that can accrue due to true stochastic sampling are reduced. Furthermore, the point spread function (PSF) of such pseudo-random undersampling schemes is incoherent [17], imparting some immunity to motion and abrupt signal changes as a function of time.

Figure 1 depicts the DISCO-DCE acquisition scheme and the k-space segmentation employed in our breast DCEMRI acquisitions. The innermost region A is fully sampled while the middle annulus B is under-sampled trifold as  $B_1$ ,  $B_2$  and  $B_3$ . The relative fractional sizes of A and  $B_i$  are 0.16 and  $(1-0.16)/3 = 0.28$  respectively. An outermost annulus C is added for high spatial resolution imaging with the number of samples in (A + B)  $1/6^{\text{th}}$  of that of (A+B+C). Following a high spatial resolution pre-contrast acquisition (A + B+C) of 120s, dynamic phases were acquired for approximately 120s using an acquisition schedule of  $AB_1AB_2AB_3\dots$  during and after injection of Gadolinium contrast. At each time point, the acquired k-space data  $AB_i$  was combined with the outermost annulus (C) from the pre-contrast phase and the missing  $B_i$  regions shared from the neighboring time points to yield full k-space data at that time point. The duration of (A+B) is  $1/6^{\text{th}}$  of that of (A+B+C) or  $120/6 = 20$ s. The duration of  $A+B_i$  (i.e. effective temporal resolution) which comprises an A region and one  $B_i$  region is given by  $(0.16*20+0.28*20)$  or 9s. This translates to 15 reconstructed dynamic phases with  $\sim 9$ s temporal resolution over the 2 minute period with lower spatial resolution. Ignoring the C region, which is pre-contrast and should not contribute to any dynamic information, the temporal footprint of each dynamic phase was  $3*(A+B_i) = 27$ s. Following the dynamic phases, 3–4 high spatial resolution 120s datasets (ABC) were acquired during the contrast washout phase. Note that  $1/6^{\text{th}}$  of the full k-space data roughly translates to a  $\sqrt{1/6} = 2.4\text{X}$  increase in voxel size along y and z dimensions for the dynamic acquisitions.

The DISCO k-space segmentation scheme was incorporated into a dual-echo bipolar-readout 3D RF-spoiled gradient echo (SPGR) sequence. A 2-point Dixon reconstruction with a region-growing based fat-water separation method proposed in [13] was used for fat-water separation at 3T. The use of high receiver bandwidths ( $\pm 167$  kHz) enabled the acquisition of opposed-phase and in-phase echoes at approximately 1.2 ms and 2.4 ms in a single TR (4.6 ms), greatly reducing scan times and enabling reliable fat-water separation. An 80% fractional echo ( $k_x$ ) readout was used to achieve the ideal Dixon TE times whilst allowing adequate spatial resolution along  $k_x$ . Self-calibrated hybrid space parallel imaging (ARC) was employed to further reduce scan times [18]. Following ARC parallel imaging reconstruction (and view sharing for the dynamic phases as described above), full k-space in-phase and opposed-phase complex images were available at each reconstructed time point. The Dixon reconstruction algorithm with a phase correction as described in [13] then generated fat-only and water-only image volumes at each reconstructed phase. All reconstruction algorithms were implemented on-line on the vendor-supplied (GE Healthcare) 8-processor (2.4 GHz) cluster to minimize image reconstruction latency. Temporal phases are reconstructed serially, as soon as the necessary k-space regions ( $A+B_i$ ) for each phase are available, resulting in a latency of approximately 60s per phase (the time to accumulate k-space data for a view shared  $A+B_i$  reconstruction is 27s)

## Human imaging

Human experiments were conducted in HIPAA-compliant fashion with IRB approval and informed consent. Imaging parameters were as follows: 15° flip angle,  $\pm 167$  kHz receiver bandwidth, TR/TE<sub>1</sub>/TE<sub>2</sub> 4.6/1.2/2.4 ms, 256×256×160 matrix, 28 cm FOV, 1.2 mm thick, ARC parallel imaging acceleration factor 1.4–2 along k<sub>y</sub>. The FOV and phase encoding steps were scaled by 1.2 along k<sub>y</sub>, maintaining the 1.1 mm spatial resolution whilst allowing for increased FOV in the left-right direction.

Twenty-six consecutive patients (range: 28–70 years, mean±SD: 54.3±10.9 years) referred for breast MRI were scanned on a GE 3T MR750 system (GE Healthcare, Waukesha, WI) using a 8 or a 16-channel breast array coil. Following localizer scans and standard T<sub>2</sub> weighted imaging, DISCO-DCE was run to acquire a pre-contrast phase, 15 dynamic phases and 3–4 post-contrast phases. A 0.1 mmol/kg Gadolinium-DTPA injection was administered at the rate of 2 ml/sec in about 10s followed by a 20 ml saline flush. Optionally, multiple additional pre-contrast phases (3–4) with variable flip angles were acquired for T<sub>1</sub> mapping. It is important to note that the first high spatial resolution post-contrast phase was still acquired at about 2 minutes after contrast injection (facilitated by the fact that our k-space ordering is true elliptical centric), in agreement with our current clinical protocol, and ACR recommendations. This is also in accordance with the findings of Nunes et al [19] who have shown that the optimal time for acquisition of post-contrast images for optimal delineation of structural features is between 90 and 270 seconds post injection of contrast for breast imaging.

## Data analysis

The current clinical protocol at our institution uses a low spatial resolution (1.1×2.5×4 mm<sup>3</sup>), fully-sampled dual-echo 9s acquisition for the dynamic phases (VIBRANT-FLEX), switching to a higher spatial resolution version (1.1×1×1.2 mm<sup>3</sup>) of the same sequence post contrast. We compared 14 patients scanned using this protocol to contrast-enhanced DISCO-DCE dynamic images obtained on 14 *different* patients with untreated breast cancer. From the 26 patients scanned using DISCO-DCE, we picked 14 patients where enhancing lesions were seen and found matching patients who were scanned using conventional VIBRANT-FLEX with the following criteria- age was matched to within 3 years, tumor size to within 5 mm. In addition, the T-grade for tumors being compared was matched. Qualitative metrics such as prevalence of artifacts and sharpness of the lesion in the dynamic images were considered.

A breast radiologist (JAL) with more than eight years experience in breast radiology blinded to the type of acquisition ranked images of each tumor according to perceived sharpness and detail from 1 = blurriest image to 28 = sharpest image. A Mann Whitney U test was used to determine statistical significance (Vassar Stats, <http://www.vassarstats.net>). In order to quantify any differences in temporal characteristics possibly introduced from DISCO view sharing, we also compared the initial slope of enhancement in the distal aortic signal enhancement curves from both protocols. The maximum slope of enhancement between two successive time points from the first 4 time points was used.

## Results

Figure 2a shows 16 temporal phases of the same section (zoom of white inset in Figure 2b) acquired using DISCO-DCE on a patient with an invasive ductal carcinoma. The first (pre-contrast) phase and the last phase were high spatial resolution ( $1.1 \times 1.1 \times 1.2 \text{ mm}^3$ , 120s per slab) while the intervening phases were high temporal resolution ( $\sim 9\text{s}$  per slab). Figure 2b shows a representative section from the acquired axial slab illustrating the excellent spatial resolution and uniform fat suppression of the 3D SPGR-Dixon technique. Figure 2c shows the enhancement curves from two different regions of interest (ROIs) inside the heterogeneously enhancing tumor (red and blue circles in Figure 2b) demonstrating the high temporal resolution of DISCO as well as the ability to seamlessly combine low and high spatial resolution data for post-processing.

In Figure 3, dynamic images from conventional low spatial resolution acquisition (a,c) and DISCO-DCE (b,d) on four *different* patients with invasive ductal carcinoma are shown. For each pair, patients matched for age, tumor size and type were chosen. The total acquisition time for both methods was  $\sim 9\text{s}$  with DISCO-DCE employing view sharing and keyhole reconstruction to generate the dynamic images and the conventional images reconstructed with zero-filling. Note the improved spatial resolution and reduced blurring and ringing artifacts in the DISCO-DCE images. The average ranking of DISCO-DCE cases (19.5) was significantly higher than that of the fully-sampled low spatial resolution cases (9.5) (Mann Whitney U test:  $U_a = 168$ ,  $z = -3.19$ , two-tailed  $p = 0.0014$ ) and is illustrated in Figure 4. Figure 5 shows the relative signal enhancement (post contrast/pre contrast) for the distal aorta as a function of time of contrast arrival in the aorta for the conventional sequence (left) and the DISCO-DCE sequence (right). Qualitatively, the curves using both techniques display very similar wash-in and wash-out characteristics. There was no significant difference in the maximum initial slope (two tailed t-test,  $p = 0.57$ ) between the two methods.

Figure 6 shows a multifocal Nottingham grade 2 invasive ductal carcinoma, demonstrating the full scope of the DISCO-DCE acquisition technique. The initial slope of contrast enhancement was estimated by fitting the first 4 time points corresponding to a total of 32 seconds as contrast reached the breast, using a linear least-squares regression. A color map of this fit was then fused to a grey-scale volume rendering of the first high-resolution post contrast scan, corresponding to  $\sim 120$  seconds after injection. This clearly shows the high spatial resolution of the post-contrast acquisition and uniform fat suppression, as well as rapid contrast enhancement in many small satellite foci (solid arrows), and a likely metastatic axillary lymph node (dashed arrow). Note that the use of Dixon fat-water separation provides excellent fat suppression in the axillary region, where conventional fat suppression is suboptimal. Pharmacokinetic modeling was performed on images acquired from a patient with invasive ductal carcinoma. Figure 7 shows the  $K_{\text{trans}}$  and  $k_{\text{ep}}$  maps (right column) generated using the 19 phases of the DISCO-DCE acquisition. The pre-contrast and post-contrast high-spatial-resolution images are shown on the left column for comparison. The heterogeneous nature of the enhancement and the good spatial resolution of the parametric maps can be clearly visualized.

## Discussion

We have developed and tested a new robust sequence for variable spatio-temporal resolution DCE MRI and demonstrated it on patients with breast cancer. A near-isotropic  $1.1 \times 1.1 \times 1.2$  mm<sup>3</sup> resolution was achieved for the high spatial resolution scans while the dynamic scans were of 9s temporal resolution with approximately  $\sqrt{6}$  or 2.4X increase in voxel size along y and z. We achieved the overall goal of an ACR-compliant high spatial resolution breast-MR acquisition with additional rapid imaging of initial contrast uptake for accurate measurement of dynamic features such as contrast arrival times and slope of maximum enhancement. Using a “one-touch” technique, we eliminated delays in switching between acquisitions, potential patient movement due to perceived end of scan and quantification errors from differing prescan parameters. The DISCO-DCE dynamic images were significantly sharper than the low spatial resolution fully-sampled VIBRANT-FLEX dynamic images, with the tumor margins and spiculations more closely resembling the high spatial resolution images.

The DISCO k-space segmentation scheme bears some similarity to the recently proposed TWIST technique [20], which has been applied to renal imaging [21] and breast DCEMRI [22]. DISCO employs variable density under-sampling i.e. increasing under-sampling factors away from the center of k-space and is capable of achieving higher acceleration factors than the spiral in- spiral out sampling scheme of TWIST. Unlike TWIST, where the k-space radius  $k_r$  of the acquired k-space points oscillates (outward to inward and back) as a function of time within each temporal phase, it monotonically increases from the center-out in DISCO, making it more ideal for capture of contrast kinetics as it is closer to true elliptical centric k-space segmentation. Furthermore, the method of Herrmann et al. [22] used a mask subtraction scheme in the breast to eliminate fat, which is suboptimal for breath-holding applications. Even in breast imaging with relatively minimal motion, this method required a retrospective image registration scheme to minimize motion artifacts.

This preliminary analysis had some limitations. We scanned a small set of patients (n=26) to assess the feasibility and image quality of our technique. Dynamic phase DISCO-DCE images from a smaller subset of 14 patients with untreated breast cancer were compared to dynamic images from a conventional low spatial resolution sequence acquired on *different* patients with tumors matched for size, type and age. This was because it is not possible to acquire the dynamic data using both techniques on the same patient without having to image twice with Gadolinium contrast injection. Even a second injection on the same patient might still carry variability due to varying contrast dynamics and patient misregistration. Using a larger number of patients could allow better matching of lesions for a more diagnostic comparison. The quantitative slope comparison was performed on the distal aorta. While it would be desirable to compare the lesion enhancement characteristics between the two dynamic sequences, it is a potentially unreliable comparison because the lesions were not identical in each group and there may be substantial variability in the degree of enhancement across tumor types even using the same technique.

There is still some minor residual blurring in rapidly enhancing masses compared to the fully sampled high spatial resolution k-space data, presumably due to signal discontinuities

in outer k-space from view sharing. However, the enhancement characteristics are still well preserved as highlighted by the sharp aortic enhancement curves. The use of view sharing makes techniques like DISCO and TWIST susceptible to motion as well as temporal blurring, especially in small lesions where the k-space energy is more dispersed. In our technique, the use of view sharing resulted in an increase in voxel size by a factor of 2.4 along y and z dimensions. This is the worst-case scenario with the assumption that signal energy is spread uniformly across k-space, an assumption true only for point objects. In practice, the larger the lesion size, the lesser the extent of blurring due to view sharing. While the maximum slope of signal enhancement is not significantly different in the two methods, the effect of view sharing on complex pharmacokinetic modeling has to be assessed and is currently underway.

The use of Dixon fat-water separation in conjunction with DISCO makes it ideal for applications like breast imaging, where fat suppression is especially challenging due to  $B_0/B_1$  heterogeneity. The algorithm can occasionally mis-assign water and fat causing fat-water swaps, particularly in regions where the phase estimation is poor or where there is aliasing. The DIXON method also restricts the echo times to 1.1/2.2 ms, which in turn limits the spatial resolution, especially along the readout direction. Using echo times of 2.2/3.3 ms or a unipolar readout could enable higher spatial resolution but at the cost of increased TR, which will require higher parallel imaging acceleration factors to maintain temporal resolution.

Future investigations include comparing view sharing with a compressed sensing (CS) based reconstruction to further reduce the temporal footprint of the temporal phases and eliminate any blurring/ghosting artifacts derived from view-sharing and keyhole reconstruction. The pseudo-random undersampling in DISCO-DCE results in an incoherent point spread function (PSF) and is ideal for combination with CS. However, CS techniques might significantly increase the reconstruction time of high-resolution breast images and would require additional computational hardware for practical reconstruction times. The incoherent nature of the DISCO PSF [17] would also disperse motion artifacts in much the same way as undersampling artifacts are dispersed in radial imaging and may provide some immunity to motion and fast signal changes.

In conclusion, the DISCO-DCE technique allows acquisition of 3D volumes during the wash-in phase with an effective temporal resolution of 9 seconds while providing adequate image quality to generate pharmacokinetic maps as well as high spatial resolution (~1mm isotropic) images during the post-contrast phase. The entire scan is performed using a single sequence, reducing scan times and ensuring that calibration prescan parameters are unchanged between the dynamic and post-contrast phases.

## Acknowledgments

Grant support: NIH R01-EB009055 and P41-RR009784



## References

1. Kuhl CK, Schild HH, Morakkabati N. Dynamic bilateral contrast-enhanced MR imaging of the breast: trade-off between spatial and temporal resolution. *Radiology*. 2005; 236:789–800. [PubMed: 16118161]
2. Goto M, Ito H, Akazawa K, et al. Diagnosis of breast tumors by contrast enhanced MR imaging: comparison between the diagnostic performance of dynamic enhancement patterns and morphologic features. *J Magn Reson Imaging*. 2007; 25:104–112. [PubMed: 17152054]
3. van Vaals JJ, Brummer ME, Dixon WT, et al. "Keyhole" method for accelerating imaging of contrast agent uptake. *J Magn Reson Imaging*. 1993; 3:671–675. [PubMed: 8347963]
4. Plewes DB, Bishop J, Soutar I, Cohen E. Errors in quantitative dynamic three-dimensional keyhole MR imaging of the breast. *J Magn Reson Imaging*. 1995; 5:361–364. [PubMed: 7633115]
5. Korosec FR, Frayne R, Grist TM, Mistretta CA. Time-resolved contrast-enhanced 3D MR angiography. *Magn Reson Med*. 1996; 36:345–351. [PubMed: 8875403]
6. Madhuranthakam AJ, Hu HH, Barger AV, Haider CR, Kruger DG, Glockner JF, Huston J 3rd, Riederer SJ. Undersampled elliptical centric view-order for improved spatial resolution in contrast-enhanced MR angiography. *Magn Reson Med*. 2006; 55(1):50–58. [PubMed: 16315207]
7. Mistretta CA, Wieben O, Velikina J, Block W, Perry J, Wu Y, Johnson K, Wu Y. Highly constrained backprojection for time-resolved MRI. *Magn Reson Med*. 2006; 55(1):30–40. [PubMed: 16342275]
8. Dougherty L, Isaac G, Rosen MA, Nunes LW, Moate PJ, Boston RC, Schnall MD, Song HK. High frame-rate simultaneous bilateral breast DCE-MRI. *Magn Reson Med*. 2007; 57:220–225. [PubMed: 17152087]
9. Ramsay E, Cause P, Hill K, Plewes D. Adaptive Bilateral Breast MRI Using Projection Reconstruction Time-Resolved Imaging of Contrast Kinetics. *J. Mag Res Imag*. 2006; 24:617–624.
10. Turnbull LW. Dynamic contrast-enhanced MRI in the diagnosis and management of breast cancer. *NMR Biomed*. 2009; 22:28–39. [PubMed: 18654999]
11. Dixon WT. Simple proton spectroscopic imaging. *Radiology*. 1984; 153:189–194. [PubMed: 6089263]
12. Reeder SB, Markl M, Yu H, Hellinger JC, Herfkens RJ, Pelc NJ. Cardiac CINE imaging with IDEAL water-fat separation and steady-state free precession. *J Magn Reson Imaging*. 2005; 22:44–52. [PubMed: 15971192]
13. Ma J. Breath-hold water and fat imaging using a dual-echo two-point Dixon technique with an efficient and robust phase-correction algorithm. *Magn Reson Med*. 2004; 52:415–419. [PubMed: 15282827]
14. Pinker K, Grabner G, Bogner W, Gruber S, et al. A combined high temporal and high spatial resolution 3 Tesla MR imaging protocol for the assessment of breast lesions. *Invest. Radiol*. 2009; 44:553–558. [PubMed: 19652611]
15. Saranathan, M.; Hargreaves, BA.; Moran, CJ.; Daniel, BL. Variable-resolution dynamic contrast enhanced breast MRI acquisition. In Proceedings of the 19th Annual Meeting of ISMRM; Montreal, Canada. 2011. (abstract 3087)
16. Saranathan M, Rettmann DW, Hargreaves BA, Clarke SE, Vasanawala SS. Differential subsampling with cartesian ordering (DISCO): A high spatio-temporal resolution Dixon imaging sequence for multiphasic contrast enhanced abdominal imaging. *J Magn Reson Imaging*. 2012; 35:1484–1492. [PubMed: 22334505]
17. Saranathan, M.; Rettmann, DW.; Hargreaves, BA.; Lipson, JA.; Daniel, BD. High Spatio-Temporal Resoluton Breast Dynamic Contrast Enhanced MRI at 3T. Proceedings of the 20th Annual meeting of ISMRM; Melbourne. 2012. (Abstract p456)
18. Beatty, PJ.; Brau, AC.; Chang, S., et al. A method for autocalibrating 2-D accelerated volumetric parallel imaging with clinically practical reconstruction times. Proceedings of the 15th Annual Meeting of ISMRM; Berlin, Germany. 2007. (abstract 1749)
19. Nunes LW, Englander SA, Charfeddine R, Schnall MD. Optimal post-contrast timing of breast MR image acquisition for architectural feature analysis. *J Magn Reson Imaging*. 2002; 16:42–50. [PubMed: 12112502]

20. Vogt, FM.; Eggebrecht, H.; Laub, G., et al. High spatial and temporal resolution MRA (TWIST) in acute aortic dissection. Proceedings of the 15th Annual Meeting of ISMRM; Berlin, Germany. 2007. (abstract 92)
21. Song T, Laine AF, Chen Q, et al. Optimal k-space sampling for dynamic contrast-enhanced MRI with an application to MR renography. *Magn Reson Med*. 2009; 61:1242–1248. [PubMed: 19230014]
22. Herrmann KH, Baltzer PA, Dietzel M, Krumbein I, Geppert C, Kaiser WA, Reichenbach JR. Resolving arterial phase and temporal enhancement characteristics in DCE MRI at high spatial resolution with TWIST acquisition. *J Magn Reson Imaging*. 2011; 34:973–982. [PubMed: 21769981]

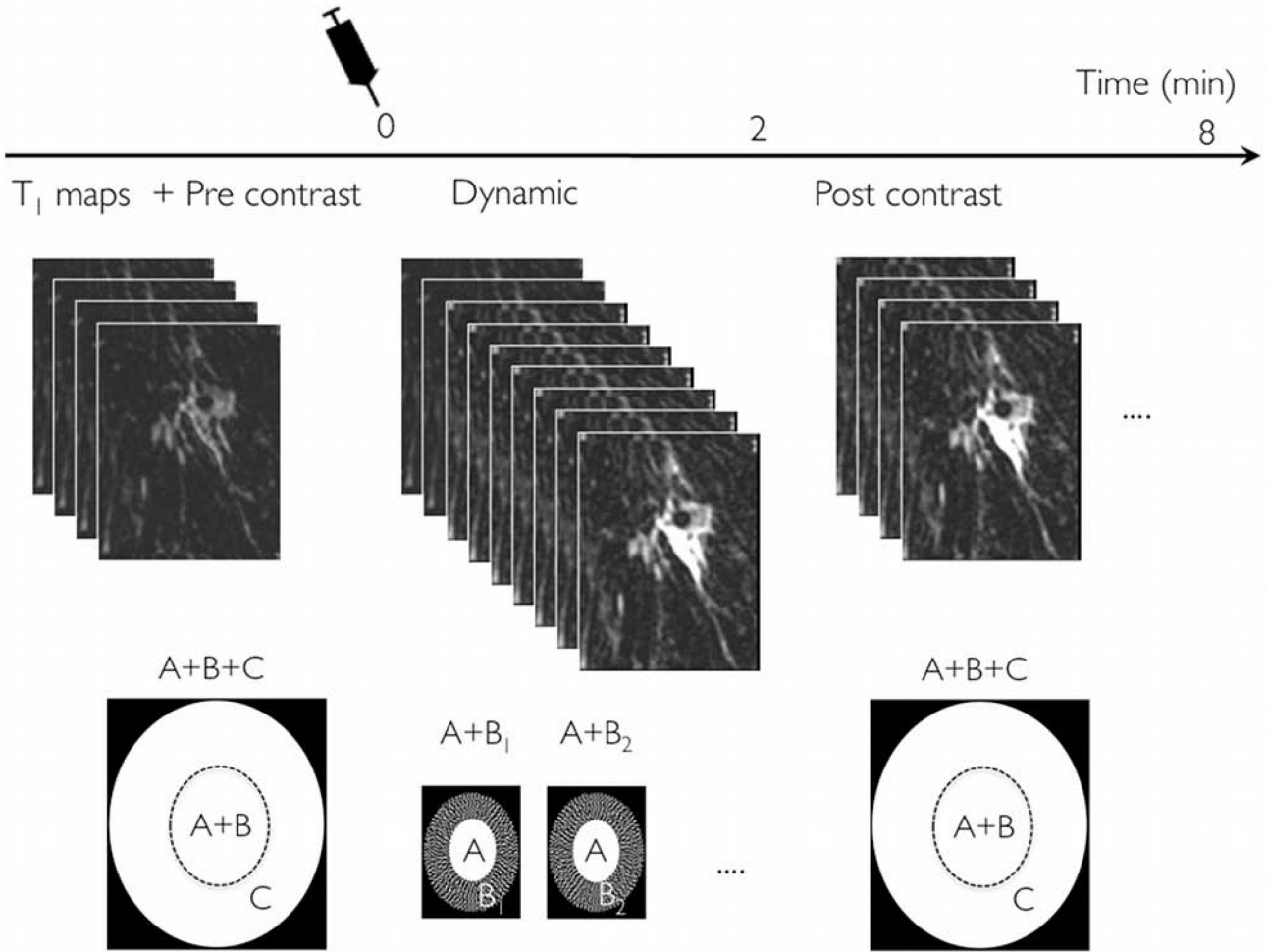


**Figure 1.**

DISCO region-scheduling and k-space segmentation scheme. A high spatial resolution pre-contrast acquisition is acquired covering the entire k-space, with optional variable flip angle data acquired for T<sub>1</sub> mapping. Following injection of Gadolinium contrast, dynamic images with 9s temporal resolution are acquired over a period of 2 minutes. Only a part of k-space is acquired for each dynamic phase, which are then reconstructed using viewsharing.

Following this dynamic acquisition, 3-4 post-contrast phases are acquired with high spatial resolution to complete the study.

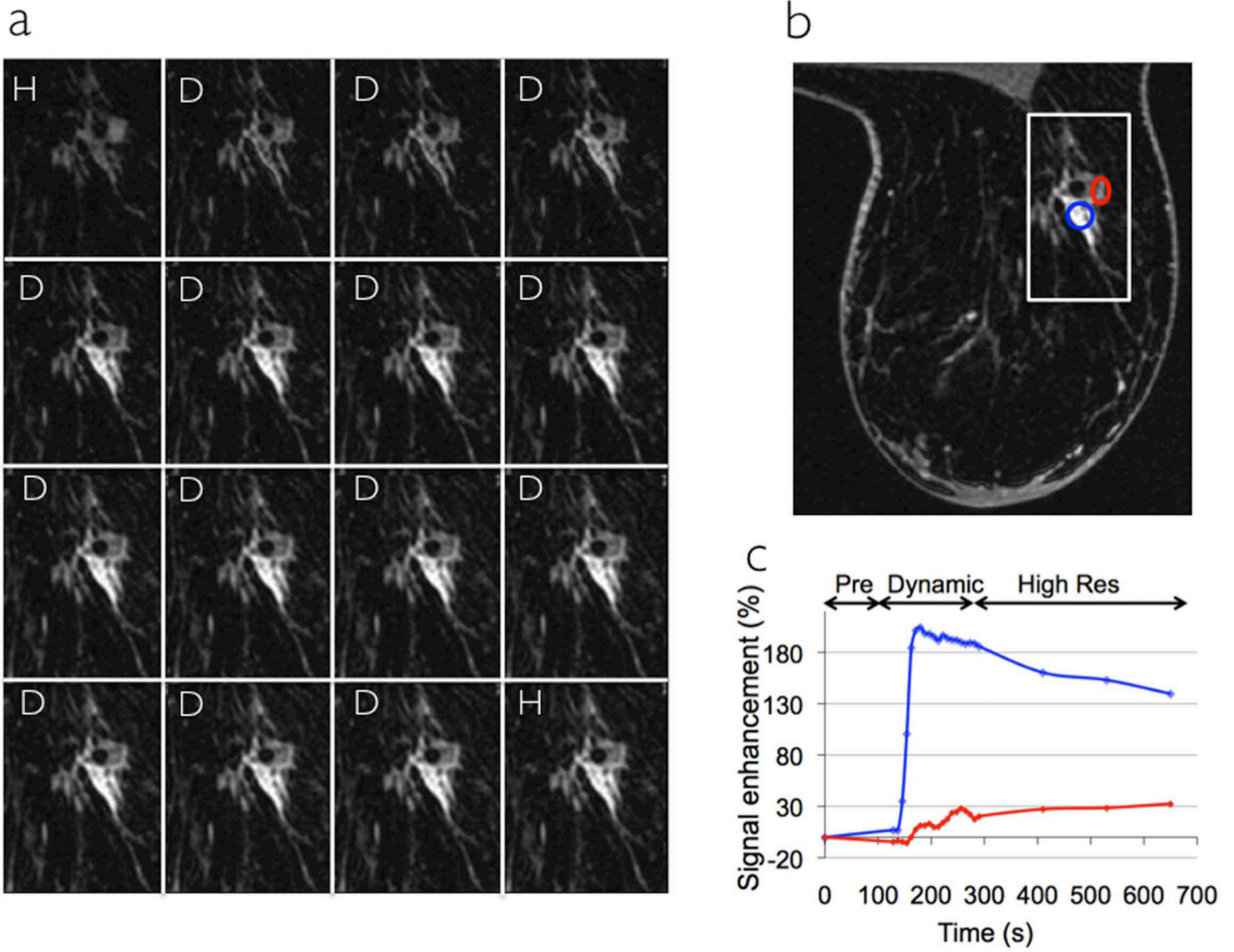


**Figure 2.** Sixteen phases (a) through the tumor (zoom of white box in the axial section shown in b) acquired on a patient with an invasive ductal carcinoma using DISCO-DCE. The first phase and last phases are high spatial resolution (H) while the middle 14 phases are dynamic high temporal resolution (D). An axial section is shown in (b) showing the ROIs and the corresponding uptake curves for the ROIs are plotted in (c). Note the non-uniform time scale illustrating the switch between dynamic and high spatial resolution modes.

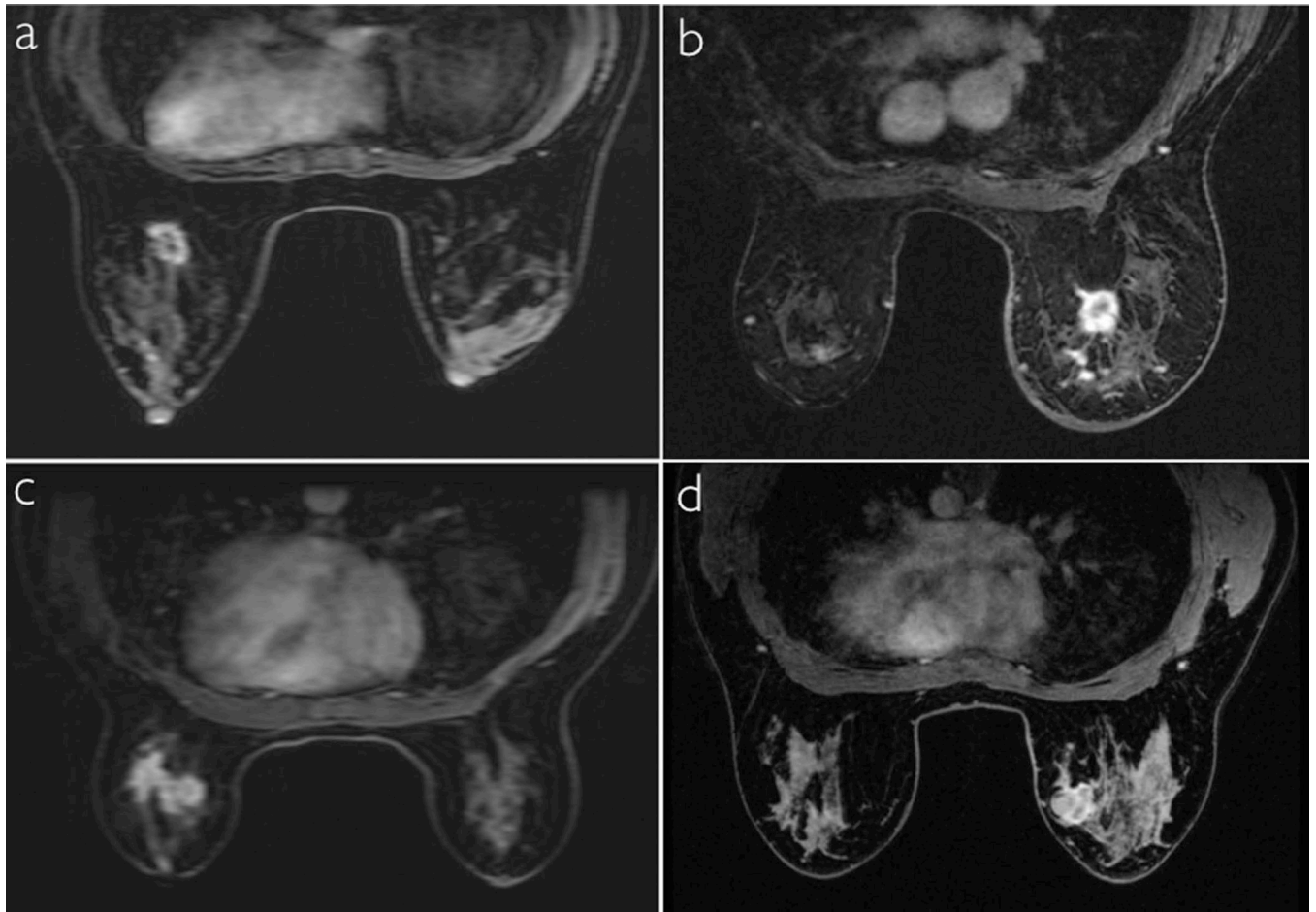


**Figure 3.** Conventional low spatial resolution VIBRANT FLEX dynamic images (a,c) and DISCO-DCE dynamic phase images (b,d) obtained with the same temporal resolution of 9s on *different* patients with breast cancer, matched for age, size, and type of tumor. Note the reduction of Gibbs ringing and blurring and improved image quality using the DISCO technique.

# Dynamic phase IQ comparison

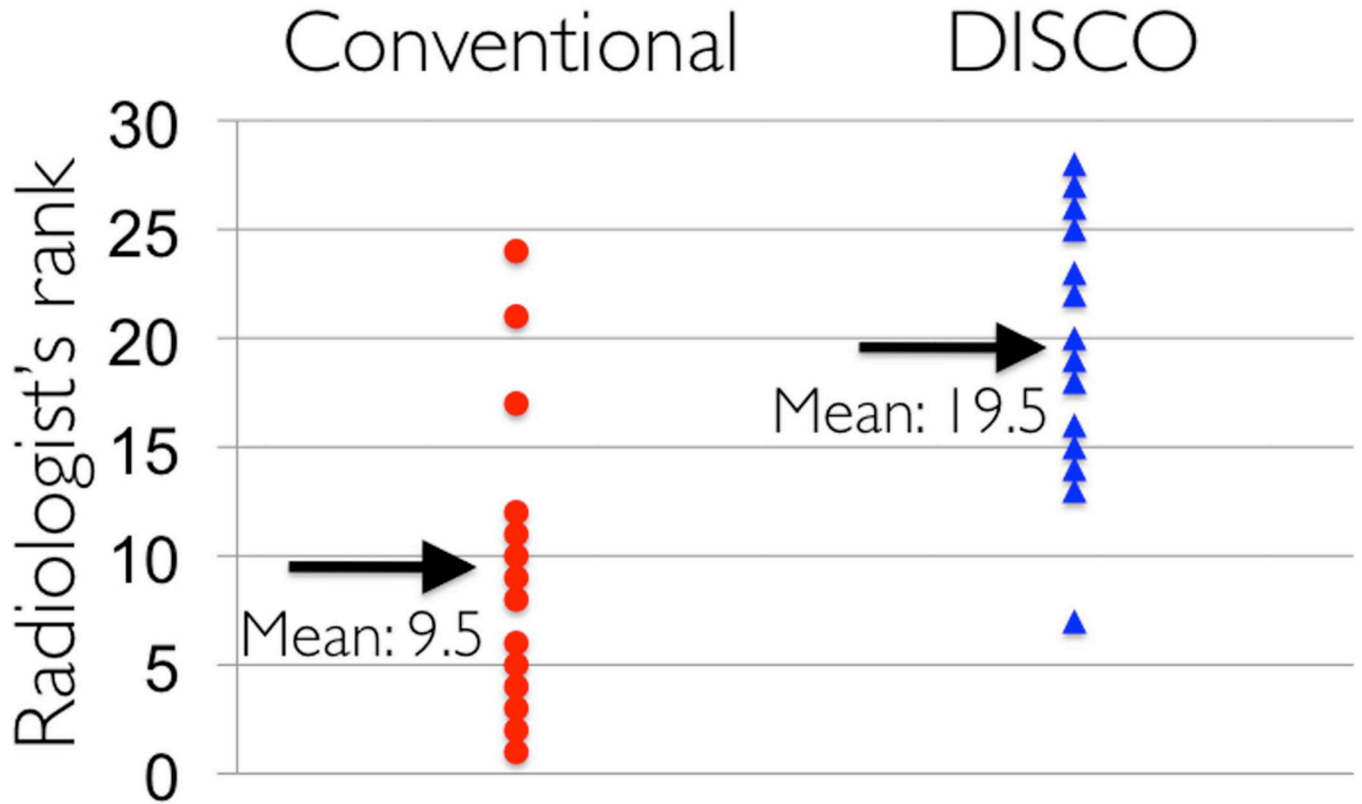


**Figure 4.** Comparison of radiologist rank ordered image scores between the conventional low spatial resolution fully sampled dynamic images and the DISCO-DCE dynamic images (both acquired with 9s temporal resolution) on 14 patients. The mean score for DISCO-DCE is significantly higher than that of the conventional dynamic images.

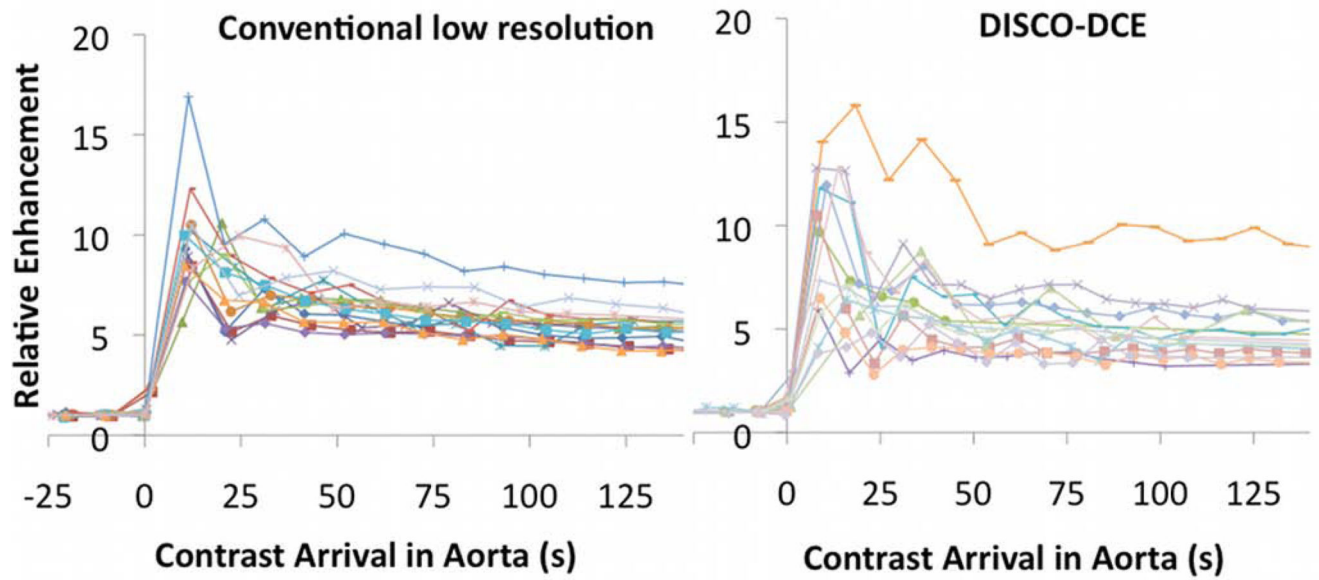


**Figure 5.**

Relative signal enhancement (post contrast/pre contrast) for the distal aorta as a function of time of contrast arrival in the aorta for the conventional dynamic sequence (left) and the DISCO-DCE dynamic sequence (right). There was no significant difference in the maximum initial slope (two tailed t-test,  $p = 0.57$ ) between the two sequences.

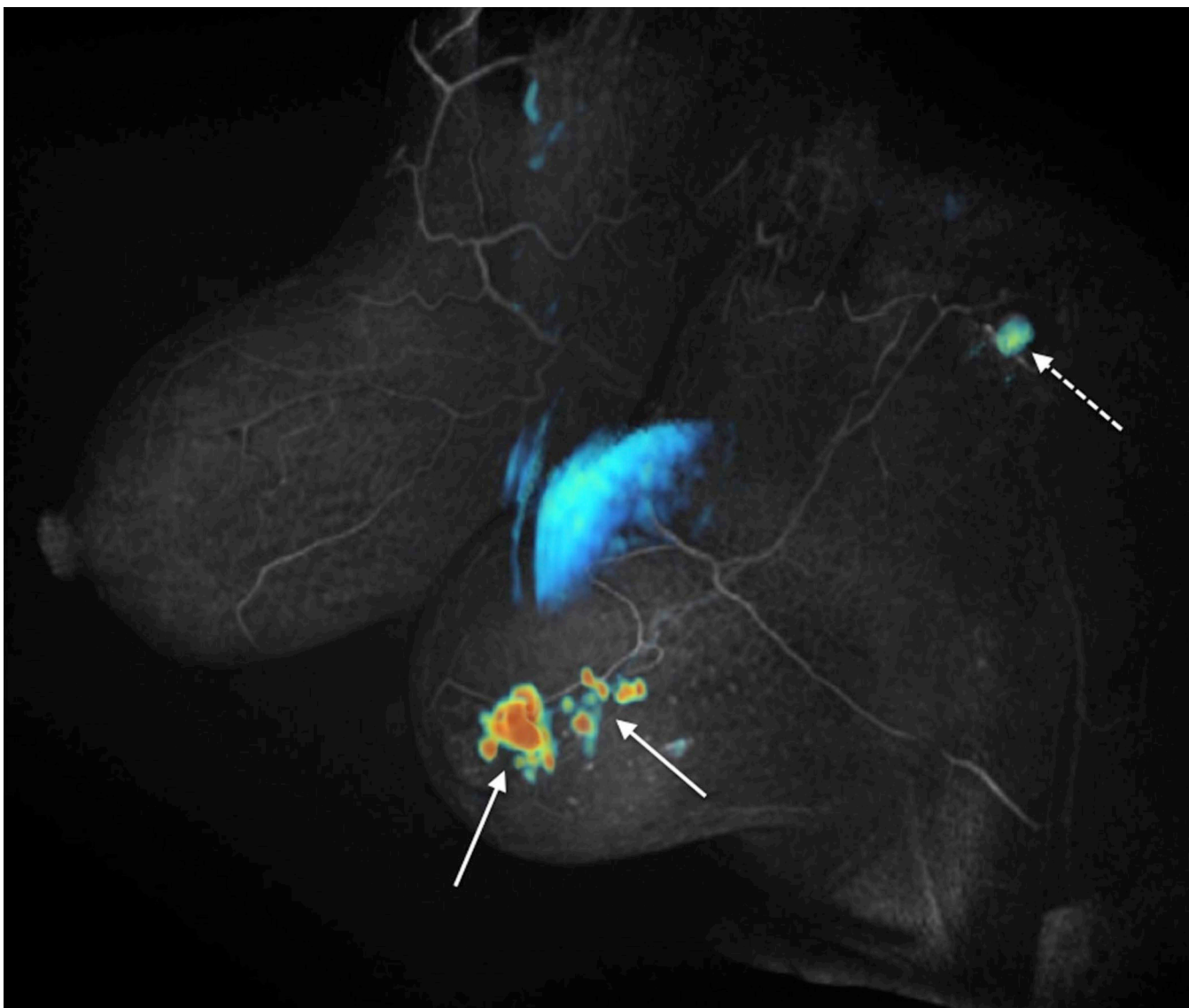


**Figure 6.** Patient with multifocal Nottingham grade 2 invasive ductal carcinoma. Grey-scale volume rendering of the first high spatial resolution post contrast scan (~120 seconds after contrast injection) with a color map of initial slope of contrast enhancement (linear regression fit of the first 4 DISCO-DCE dynamic phases) clearly depicts rapid contrast enhancement in many small satellite foci (solid arrows), and a likely metastatic axillary lymph node (dashed arrow). The large blue region in the middle of the image is part of the heart, which also enhances and is acquired as part of the axial acquisition.



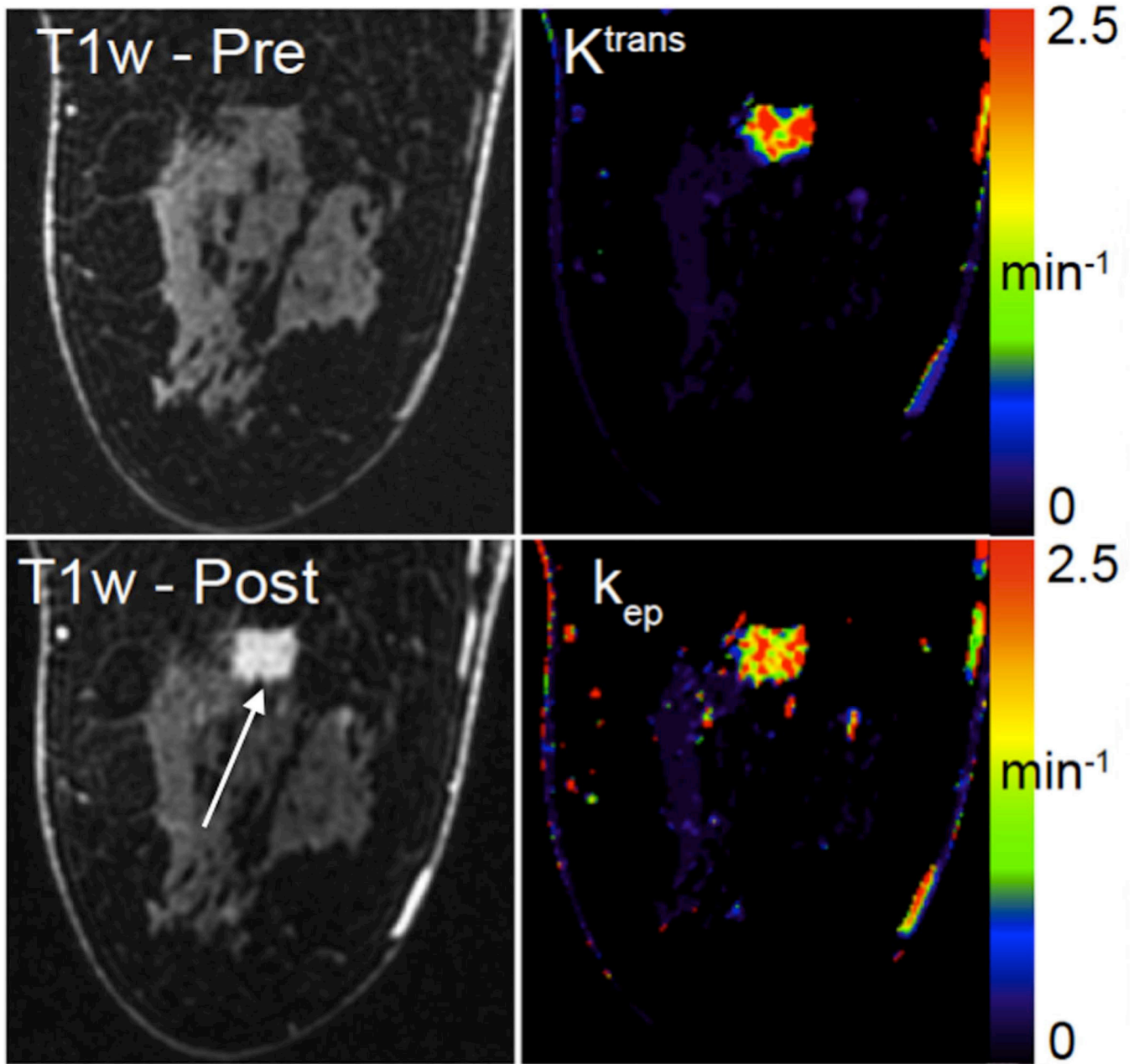


**Figure 7.**

Single slice from DISCO-DCE high-spatial-resolution pre-contrast and post-contrast phases (left column) obtained from a patient with invasive ductal carcinoma. On the right column are the pharmacokinetic maps showing  $K^{\text{trans}}$  and  $k_{\text{ep}}$  maps generated from the DISCO-DCE data acquired with 9s temporal resolution. The high spatial resolution and the heterogeneous enhancement of the tumor can be clearly visualized in the parametric maps.